

Entanglement entropy on a fuzzy sphere with a UV cutoff

Hong Zhe Chen and Joanna L. Karczmarek

*Department of Physics and Astronomy
University of British Columbia, Vancouver, Canada V6T 1Z1*

Abstract

We introduce a UV cutoff into free scalar field theory on the noncommutative (fuzzy) two-sphere. Due to the IR-UV connection, varying the UV cutoff allows us to control the effective nonlocality scale of the theory. In the resulting fuzzy geometry, we establish which degrees of freedom lie within a specific geometric subregion and compute the associated vacuum entanglement entropy. Entanglement entropy for regions smaller than the effective nonlocality scale is extensive, while entanglement entropy for regions larger than the effective nonlocality scale follows the area law. This reproduces features previously obtained in the strong coupling regime through holography. We also show that mutual information is unaffected by the UV cutoff.

1 Introduction

As a tool used to investigate phenomena from the nature of quantum criticality to the holographic origin of space time, entanglement entropy in quantum field theories has received wide interest. One of the strengths of geometric entanglement entropy (entanglement entropy associated with a particular region of space) is that its definition is independent of the details of the field theory, such as its degrees of freedom, and of the quantum state under consideration. A reflection of this universality is the simple holographic interpretation of geometric entanglement entropy as an area of a minimal surface [1].

Since entanglement entropy is universal, it is a good tool to study unconventional quantum field theories, such as those lacking in locality. Nonlocal theories have been argued to be relevant to the study of holographic duals of flat space [2], while noncommutative theories in particular have been argued to be related to black hole horizons and information scrambling [3]. Unsurprisingly, entanglement entropy in nonlocal theories can have drastically different properties than it does in local theories. For example, the now very-well established ‘area law’—in the vacuum state, the leading term of entanglement entropy grows (at most) proportionately to the area of the boundary of the region of interest— can fail if locality is not present. Studying entanglement entropy in nonlocal theories can help us understand which properties of entanglement entropy are dependent on locality and how. Conversely, detailed behaviour of entanglement entropy in nonlocal theories can illuminate features of nonlocal theories such as the presence or absence of a UV-IR connection.

Vacuum entanglement entropy in noncommutative field theories has been studied both holographically [4, 5, 6, 7] and directly [8, 9, 10, 11, 12, 13, 14]. Holographically, for regions whose size is below a certain critical length scale L_{trans} , the entanglement entropy grows with the volume of the region, while the area law is restored for regions whose dimensions are larger than the critical length scale L_{trans} . The critical length scale L_{trans} is proportional to the UV cutoff, revealing information about the UV-IR connection. It is not immediately clear whether the holographic approach is truly measuring geometric entanglement entropy in the field theory, as existence of well defined geometric regions in the nonlocal boundary theory corresponding to regions of AdS boundary is not immediately obvious. To remove these doubts, entanglement entropy was studied for a free field on a fuzzy (noncommutative) sphere directly, using a finite N matrix model [9]. However, owing to an inevitable relationship between the noncommutativity parameter $\sqrt{\theta}$, the circumference of the sphere R and the UV cutoff λ_{UV} :

$$2R^2 = N\theta \quad \text{and} \quad \lambda_{\text{UV}} = R/N, \quad (1)$$

the expected critical length scale $L_{\text{trans}} \sim \theta/\lambda_{\text{UV}}$ is larger than the radius of the sphere, making it impossible to examine regions whose dimensions larger than L_{trans} .

In this paper, we give a prescription for lowering the UV cutoff in a scalar field theory on a fuzzy sphere, increasing the associated wavelength from $\lambda_{\text{UV}} = R/N$ to $\tilde{\lambda}_{\text{UV}} = R/n$, and defining geometric regions in a theory with a UV cutoff. In this simple theory, we are able to recover the phase transition previously seen holographically, as described above.

As can be seen in Figure 1, imposing a lower UV cutoff has no effect on entanglement entropy associated with a spherical cap of angular size θ when θ is small. For larger regions, entanglement entropy becomes proportional to the length of the boundary of the region, $2\pi R \sin \theta$. As expected, this transition from extensive entanglement entropy to area law happens at an angular size θ_{trans} which increases proportionately to $1/\tilde{\lambda}_{\text{UV}} \sim n$ (Figure 3).

The rest of this paper is organized as follows. We work with a free scalar field theory on a noncommutative—or fuzzy—sphere with $R = 1$ throughout the paper. In section 2 we describe our approach to computing entanglement entropy associated with a spherical cap region in the presence of a UV cutoff. In section 3 we present detailed behaviour of the entanglement entropy as we vary θ , n , N and the mass of the scalar field. In section 4, we discuss mutual information.

2 Methodology

The Hamiltonian for a real scalar field theory on a fuzzy sphere of radius one is given by

$$H = \frac{4\pi}{N} \frac{1}{2} \text{Tr} \left((\dot{\phi})^2 - \sum_{i=1,2,3} [L_i, \phi]^2 + \mu^2 \phi^2 \right), \quad (2)$$

where ϕ is an $N \times N$ Hermitian matrix representing the scalar field, whose mass is μ . L_i generate an irreducible representation of the $\text{SU}(2)$ algebra:

$$[L_i, L_j] = \sum_k i\epsilon_{ijk} L_k, \quad \sum_{i=1,2,3} L_i^2 = (N^2 - 1)/4. \quad (3)$$

The Hamiltonian (2) represents N^2 coupled harmonic oscillators of equal masses. We work in a basis where L_3 is diagonal. In [8] it was noticed that Hamiltonian (2) is a sum of $2N + 1$ independent (mutually non-interacting) sectors. This decomposition can be viewed as a consequence of rotational symmetry. To implement it, we need to first ‘complexify’ the scalar field ϕ . The Hermitian matrix ϕ represents the configuration space of our system, \mathbb{R}^{N^2} . First, let’s repackage the information contained in ϕ to make its nature as a real vector space easier to see, by defining a real matrix $\tilde{\phi} = \frac{1}{2}(\phi + \phi^T) + \frac{1}{2i}(\phi - \phi^T)$. Matrices ϕ and $\tilde{\phi}$ are in one-to-one correspondence with each other, with $\phi = \frac{1}{2}(\tilde{\phi} + \tilde{\phi}^T) + \frac{i}{2}(\tilde{\phi} - \tilde{\phi}^T)$, and $\tilde{\phi}$ is a real matrix iff ϕ is Hermitian, thus each entry in matrix $\tilde{\phi}$ is an independent real field. The Hamiltonian (2) can be rewritten in terms of $\tilde{\phi}$,

$$H = \frac{4\pi}{N} \frac{1}{2} \text{Tr} \left(\dot{\tilde{\phi}}^T \dot{\tilde{\phi}} - \sum_{i=1,2,3} [L_i, \tilde{\phi}^T][L_i, \tilde{\phi}] + \mu^2 \tilde{\phi}^T \tilde{\phi} \right), \quad (4)$$

while the $\text{U}(N)$ invariant metric (from which the measure derives) on configuration space is given by

$$ds^2 = \text{Tr} d\phi^2 = \text{Tr} d\tilde{\phi}^T d\tilde{\phi}. \quad (5)$$

It is now easy to see that the Hamiltonian (4) contains $2N + 1$ independent sectors. In (4), consider $\tilde{\phi}$ to be a complex matrix and replace transpose with Hermitian conjugate. On real matrices $\tilde{\phi}$, the Hamiltonian is unchanged. Now, consider the action of $e^{i\alpha L_3}$ on the complexified $\tilde{\phi}$: $\tilde{\phi} \rightarrow e^{i\alpha L_3} \tilde{\phi} e^{-i\alpha L_3}$. It is easy to see that the Hamiltonian is unchanged under this action. Since under this action each term $\tilde{\phi}_{ab}$ in the complexified $\tilde{\phi}$ acquires a phase $e^{i(a-b)\alpha}$, we learn that the Hamiltonian contains terms with $(\tilde{\phi}^\dagger)_{dc} \tilde{\phi}_{ab} = \tilde{\phi}_{cd}^* \tilde{\phi}_{ab}$ only if $(a-b) - (c-d)$ is zero. Reducing $\tilde{\phi}$ back to a real matrix, we see that the Hamiltonian does indeed contain $2N + 1$ independent sectors $V^{(m)}$, each consisting of terms $\tilde{\phi}_{ab}$ with a fixed $a - b = m$, for m from $-N$ to N . We are able to compute entanglement entropy in each of those sectors separately, greatly speeding up the numerical analysis.

In each sector $V^{(m)}$, the Laplacian operator $\Delta : \tilde{\phi} \rightarrow \sum_{i=1,2,3} [L_i, [L_i, \tilde{\phi}]]$ has the non-degenerate eigenvalues $j(j+1)$ with corresponding eigenvectors $v_j^{(m)}$ for j from $|m|$ to $N-1$. To impose a UV cutoff, we focus on a subspace of $V^{(m)}$ spanned by the $n - |m|$ eigenvectors $v_j^{(m)}$ for j from $|m|$ to $n-1$. Denote such a subspace with $V_n^{(m)}$ and let $O_n^{(m)} : V^{(m)} \rightarrow V_n^{(m)}$ be a linear operator such that $O_n^{(m)}(v_j^{(m)}) = v_j^{(m)}$ for $j \in \{|m|, \dots, n-1\}$ and $O_n^{(m)}(v_j^{(m)}) = 0$ for $j \in \{n, \dots, N-1\}$. Under the natural inner product, the eigenvectors of the Laplacian are orthogonal, so we also have the transpose of $O_n^{(m)}$, $(O_n^{(m)})^T : V_n^{(m)} \rightarrow V^{(m)}$ with $(O_n^{(m)})^T(v_j^{(m)}) = v_j^{(m)}$ for $j \in \{|m|, \dots, n-1\}$. (We use a transpose rather than a Hermitian conjugate as $V^{(m)}$ and $V_n^{(m)}$ are real vector spaces.)

In [9] it was argued that the degrees of freedom associated with a spherical cap centered on the north pole are represented by matrix entries ϕ_{ab} (or $\tilde{\phi}_{ab}$) with $a + b < N(1 - \cos(\theta))$. For maximal control over selection of degrees of freedom, we define an operator Z , which ‘measures’ the position of any degree of freedom along the L_3 (or z) axis. This operator acts on any matrix entry ϕ_{ab} by multiplying it by $N + 1 - (a + b)$. When Z is restricted to a single sector $V^{(m)}$, we denote the corresponding operator $Z^{(m)}$. Thus, we can easily identify, given θ , which degrees of freedom in each sector $V^{(m)}$ are inside or outside the spherical cap. We denote with $P_\theta^{(m)}$ the operator acting on a sector $V^{(m)}$ which projects onto the degrees of freedom within a given cap (with $(P_\theta^{(m)})^2 = P_\theta^{(m)}$).

The UV cutoff is associated with a projection operator $(O_n^{(m)})^T(O_n^{(m)})$ which does not commute with $P_\theta^{(m)}$ or $Z^{(m)}$. This is not surprising, and implies that imposing a cutoff ‘blurs’ the edges of the spherical cap region. To consider a spherical cap in a theory with a UV cutoff, we can replace $P_\theta^{(m)}$ with $P_{\theta,n}^{(m)} := O_n^{(m)} P_\theta^{(m)} (O_n^{(m)})^T$, which acts on $V_n^{(m)}$. $P_{\theta,n}^{(m)}$ is not a projection operator itself. In a UV-restricted theory, we would identify degrees of freedom inside the spherical cap with an eigenspace of $P_{\theta,n}^{(m)}$ whose eigenvalues are greater than half. This is sensible as the eigenvalues of $P_{\theta,n}^{(m)}$ are between 0 and 1 by construction, with most of them close to either 0 or 1 and only a small subset falling in-between.

A better (it turns out) method to assign the degrees of freedom uses the operator $Z_n^{(m)} := O_n^{(m)} Z^{(m)} (O_n^{(m)})^T$. The inside of the spherical cap is associated with eigenvectors of $Z_n^{(m)}$ whose eigenvalues are greater than $z = (N - \frac{1}{2}) \cos \theta$. While one might think naively that methods based on operators $P_{\theta,n}^{(m)}$ and $Z_n^{(m)}$ are interchangeable (at least in the large N

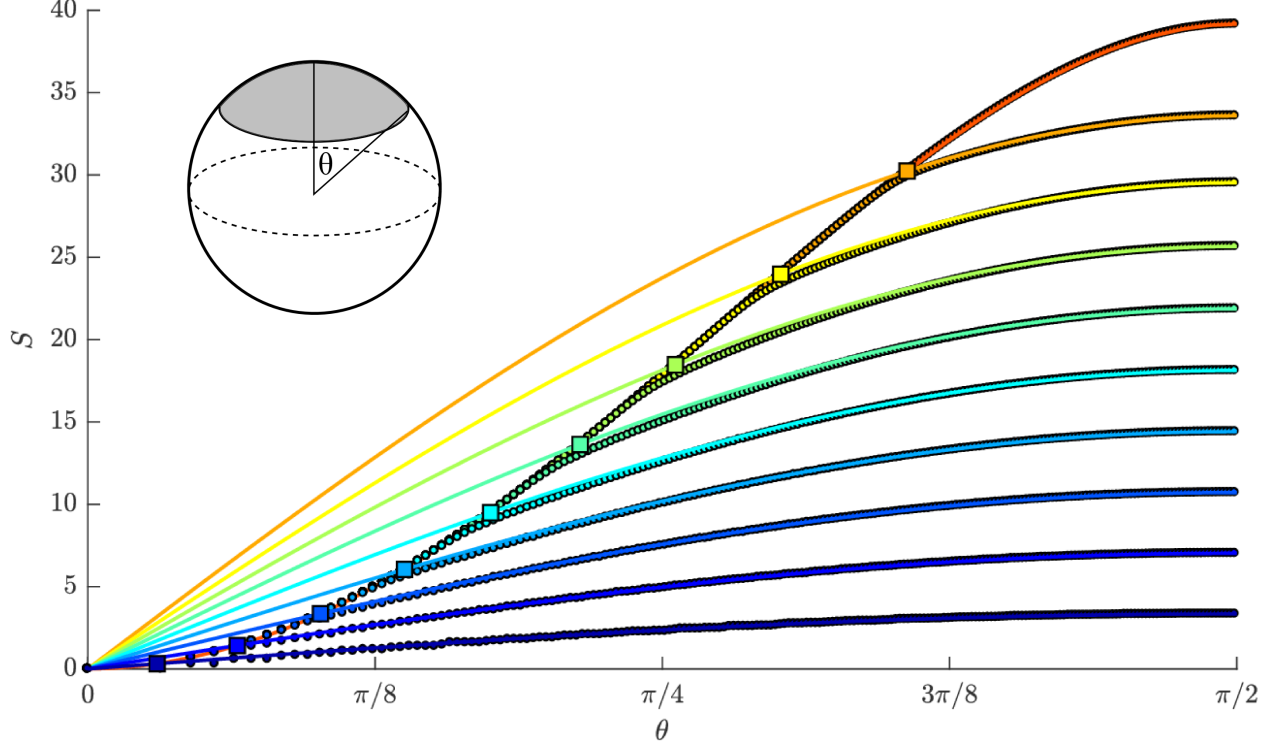


Figure 1: Entanglement entropy associated with a polar cap region against cap's angular size θ for various UV cutoffs. Here, $N = 200$, $\mu = 1$, and n takes values $20, 40, \dots, N$, indicated with colors from dark blue ($n = 20$) to redish orange ($n = N = 200$). For $n < N$, solid lines show $S(\theta = \pi/2) \sin(\theta)$, which is proportional to the length of the cap's boundary.

limit), this turns out to not be the case. While for entanglement entropy, the two methods do produce similar (though not identical) results, significant artifacts are introduced into mutual information if the operator $P_{\theta,n}^{(m)}$ is used to assign degrees of freedom belonging to a region (see section 4). This highlights the delicate nature of delineating geometric regions in a fuzzy geometry.

All the computations presented in the paper were obtained using $Z_n^{(m)}$. In each UV-controlled sector $V_n^{(m)}$, we have two self-adjoint operators, the Laplacian Δ and $Z_n^{(m)}$. If we write the Hamiltonian in the basis in which $Z_n^{(m)}$ is diagonal, we have a system of $n - |m|$ coupled harmonic oscillators. We can use well-established procedures [15, 16] for computing the entanglement entropy of a selected number of those oscillators (using the above criteria for which degrees of freedom fall inside/outside a given spherical cap).

3 Entanglement entropy

Leading order entanglement entropy of a spherical cap region on a commutative sphere is proportional to $n \sin \theta$, where n is a discretization parameter such that the total number of degrees of freedom is proportional to n^2 [10]. We can think of the discretized commu-

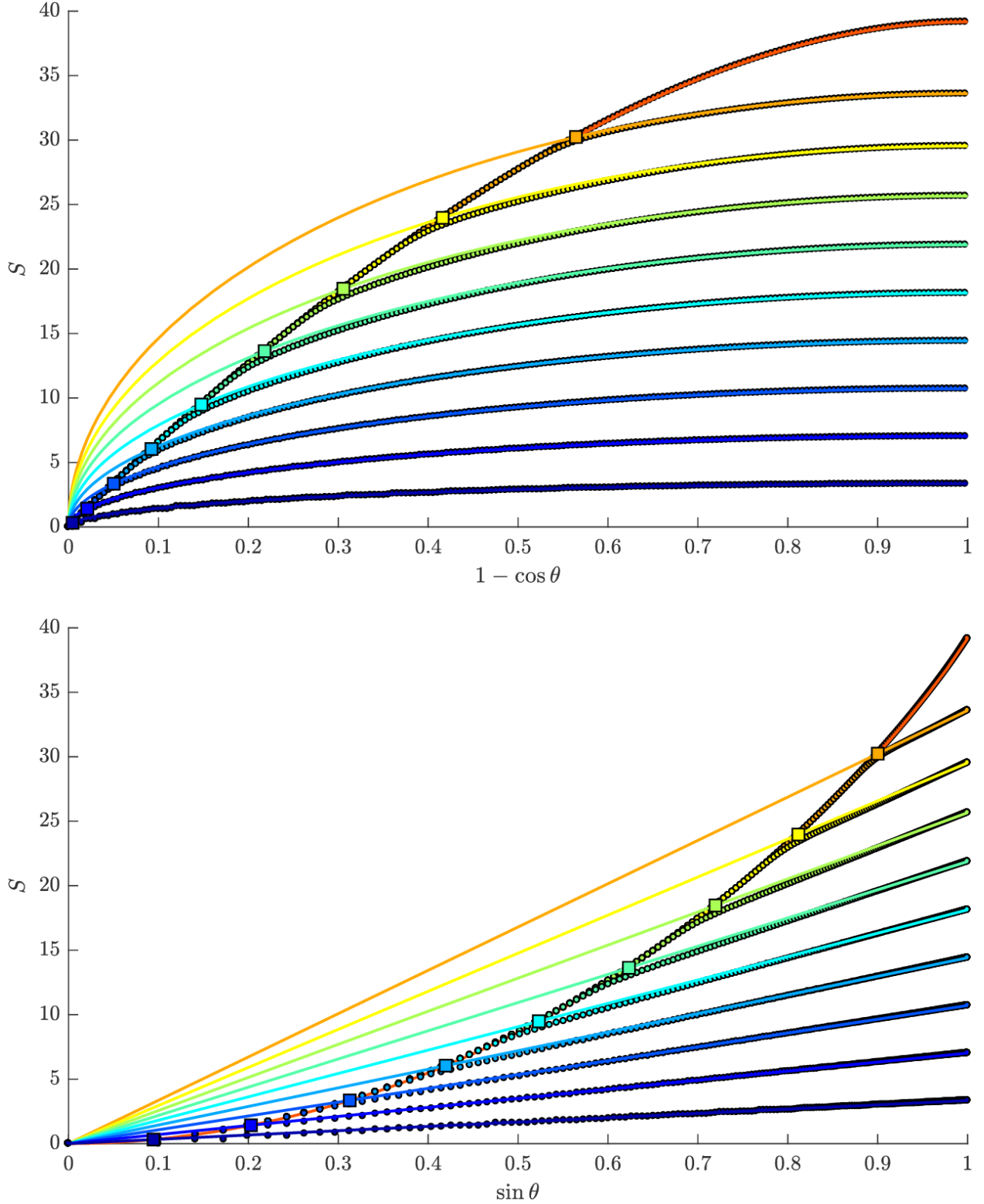


Figure 2: Entanglement entropy S of a polar cap plotted against $1 - \cos \theta$ (proportional to the area of the polar cap) and $\sin \theta$ (proportional to the length of the polar cap boundary) for $N = 200$, for the data shown in Figure 1.

tative sphere as a noncommutative sphere with N taken to infinity while n is held fixed. We introduce a notation, $S(N, n; \theta)$ for the entanglement entropy of a spherical cap in a noncommutative sphere; $S(\infty, n; \theta) = \text{const} \cdot n \sin \theta$ is then the local (commutative) result.

In Figure 1, entanglement entropy in noncommutative field theory is plotted against cap size for a selection of UV cutoff parameters n . For each value of $n < N$, a sine curve is plotted at an amplitude matching the entanglement entropy at $\theta = \pi/2$. It is clear that imposing a UV cutoff has no effect on entanglement entropy for small cap sizes, and that entanglement entropy becomes proportional to the length of the cap's boundary once the cap is large enough at a given UV cutoff. This is further highlighted in Figure 2, where the entanglement entropy is plotted as a function of the cap's area (top) and as a function of the length of the cap's boundary (bottom). At any given UV cutoff, as θ grows, there is a transition from extensive behaviour characteristic of a highly non-local theory to area-law behaviour characteristic of a local theory.

In Figures 1 and 2, we highlight the point at which this transition happens with colored squares. Since this is a smooth cross-over rather than a sharp phase transition, the exact position of the cross-over is not well defined; we choose to use the intersection between sine curves (which represent behaviour expected from a local theory) and the interpolated curve for $n = N$ (which represents nonlocal behaviour). We have computed this cross-over point as a function of the cutoff parameter n ; its roughly linear behaviour with n can be seen in Figure 3 (bottom).

This linear behaviour of the transition point between non-local and local behaviour in entanglement entropy is a clear demonstration of the UV-IR connection on the fuzzy sphere. The UV-IR connection in noncommutative theories [17] implies that for a theory with a noncommutativity scale $\sqrt{\theta}$ defined by $[x_1, x_2] = i\theta$, the nonlocality scale is $\theta/\lambda_{\text{UV}}$, where λ_{UV} is the UV cutoff wavelength. On the fuzzy sphere with radius R , we have $\theta = R^2/J$ (where $N = 2J + 1$), and the UV cutoff is $\tilde{\lambda}_{\text{UV}} = R/n$, implying that the transition should happen at $\theta_{\text{trans}} = \text{const} \cdot n/N$, consistent with the behaviour shown in Figure 3.

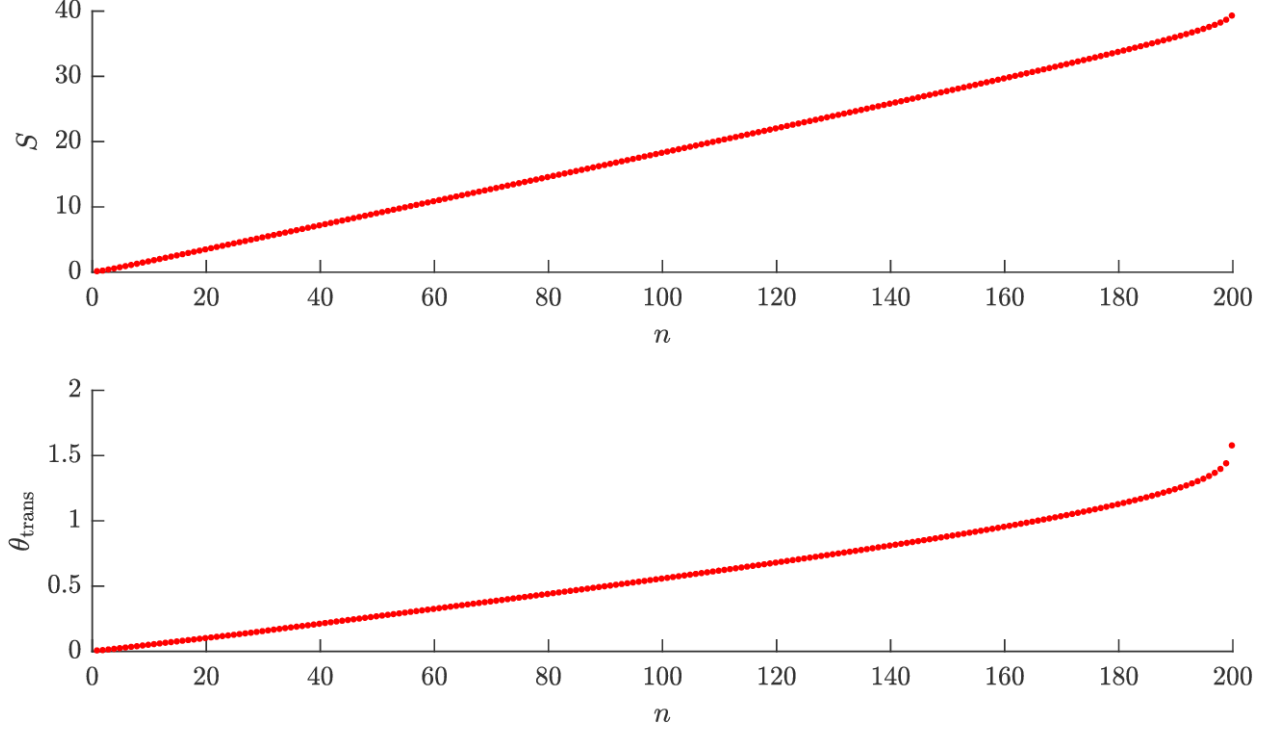


Figure 3: Entanglement entropy of a hemisphere (top) and transition angle θ_{trans} from Figure 1 (bottom) against the UV cutoff parameter n . $N = 200$, $\mu = 1$.

To examine the behaviour of entanglement entropy in more detail, we begin with dependence on the quantization parameter N . As was already observed in [9], entanglement entropy S for cap with a fixed angular size grows linearly with N . This is peculiar in a non-local theory with N^2 degrees of freedom: we could naively expect entanglement entropy to be proportional to N^2 . However, the theory's nonlocality is not complete, allowing it to reproduce the behaviour of the local theory when expected. In Figure 4, we plot $S(N, n; \theta)/N$ as a function of θ , to show that it converges to a function of n/N and θ .

Further, at a fixed N , the entanglement entropy of a hemisphere, $S(N, n, \pi/2)$, is proportional to the cutoff parameter n , as can be seen in Figure 3 (top). Together, Figures 3 and 4 establish that the entanglement entropy of any spherical cap with $\theta > \theta_{\text{trans}}$ is proportional to the UV cutoff parameter n .

Entanglement entropy for small regions is smaller than the local theory would predict. Further, for small regions, the entanglement entropy is independent of the imposed UV cutoff (though it is still proportional to N). This is a sign that only low-momentum modes participate in entanglement entropy when $\theta < \theta_{\text{trans}}$.

In summary, in the large N limit, we can write

$$S(N, n; \theta) = \begin{cases} N s_{\text{extensive}}(\theta) & \text{for } \theta < \theta_{\text{trans}}(n/N) \\ C n \sin(\theta) & \text{for } \theta > \theta_{\text{trans}}(n/N) \end{cases}, \quad (6)$$

where C is a constant, θ_{trans} is a function of n/N only, and $s_{\text{extensive}}(\theta) \sim \theta^2$ for small θ . The

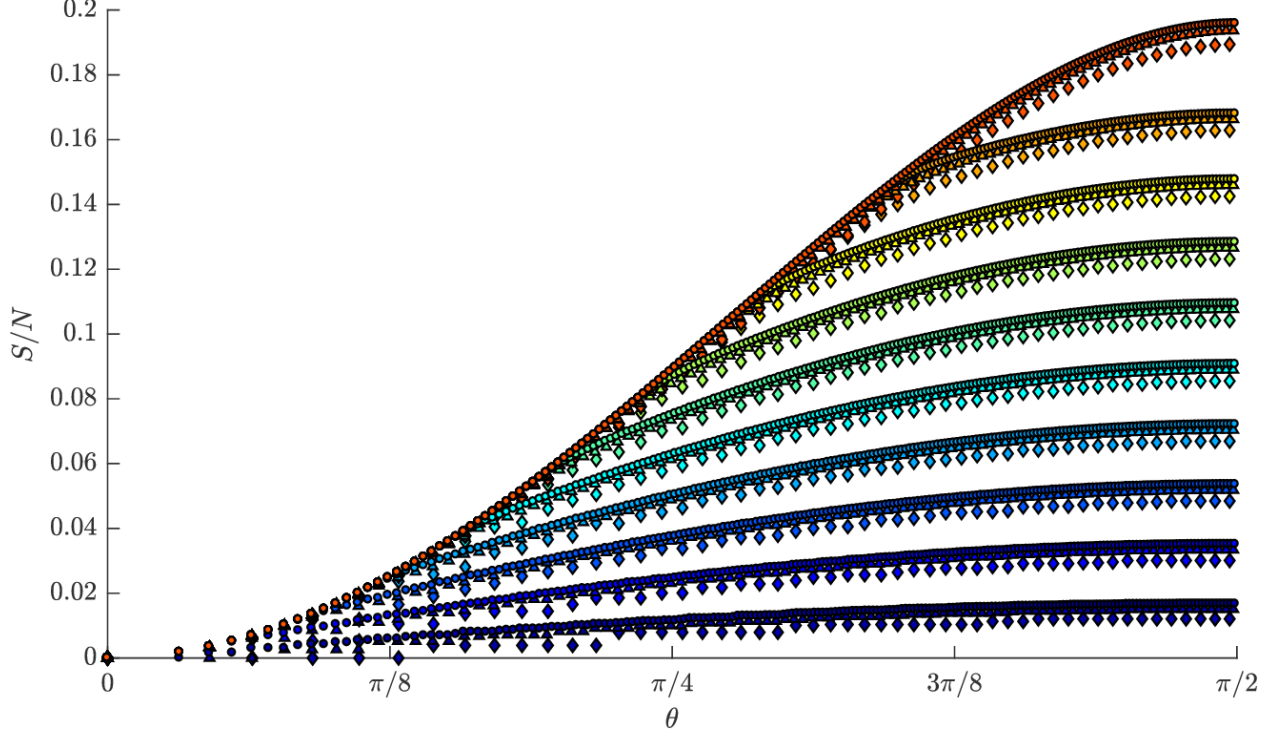


Figure 4: Entanglement entropy divided by the quantization parameter, S/N , plotted against angular cap size θ for various UV cutoffs and various N . The large diamonds, medium triangles, and small circles indicate $N = 50, 100, 200$ respectively. The UV cutoff parameters are proportional to N , and given by $n = N/10, 2N/10, \dots, N$, indicated with colors from dark blue to redish orange.

above result includes behaviour of a commutative theory, $S(\infty, n; \theta) = Cn \sin(\theta)$, since for $n/N = 0$, $\theta_{\text{trans}} = 0$.

Finally, we explore mass dependence of the entanglement entropy. In Figure 5, we show that entanglement entropy with a UV cutoff has similar behaviour to that without an imposed UV cutoff (which was discussed in [9]), being insensitive to changes in mass as long as $\mu < n$ and tending towards zero for $\mu > n$. In Figure 6, we plot S against θ for low and high masses. In the low mass case, the entanglement entropy is nearly unchanged from $\mu = 1$. In the high mass case, as the mass term dominates the kinetic energy terms, entanglement decreases, still however retaining some of the qualitative features of the intermediate mass case. Figure 7 further compares the $\mu = 1$ and $\mu = 10^{-3}$ cases. We see that the main effect of reducing the mass is a nearly-constant shift in the entanglement entropy that is the result of an appearance of a very-light mode at small mass.

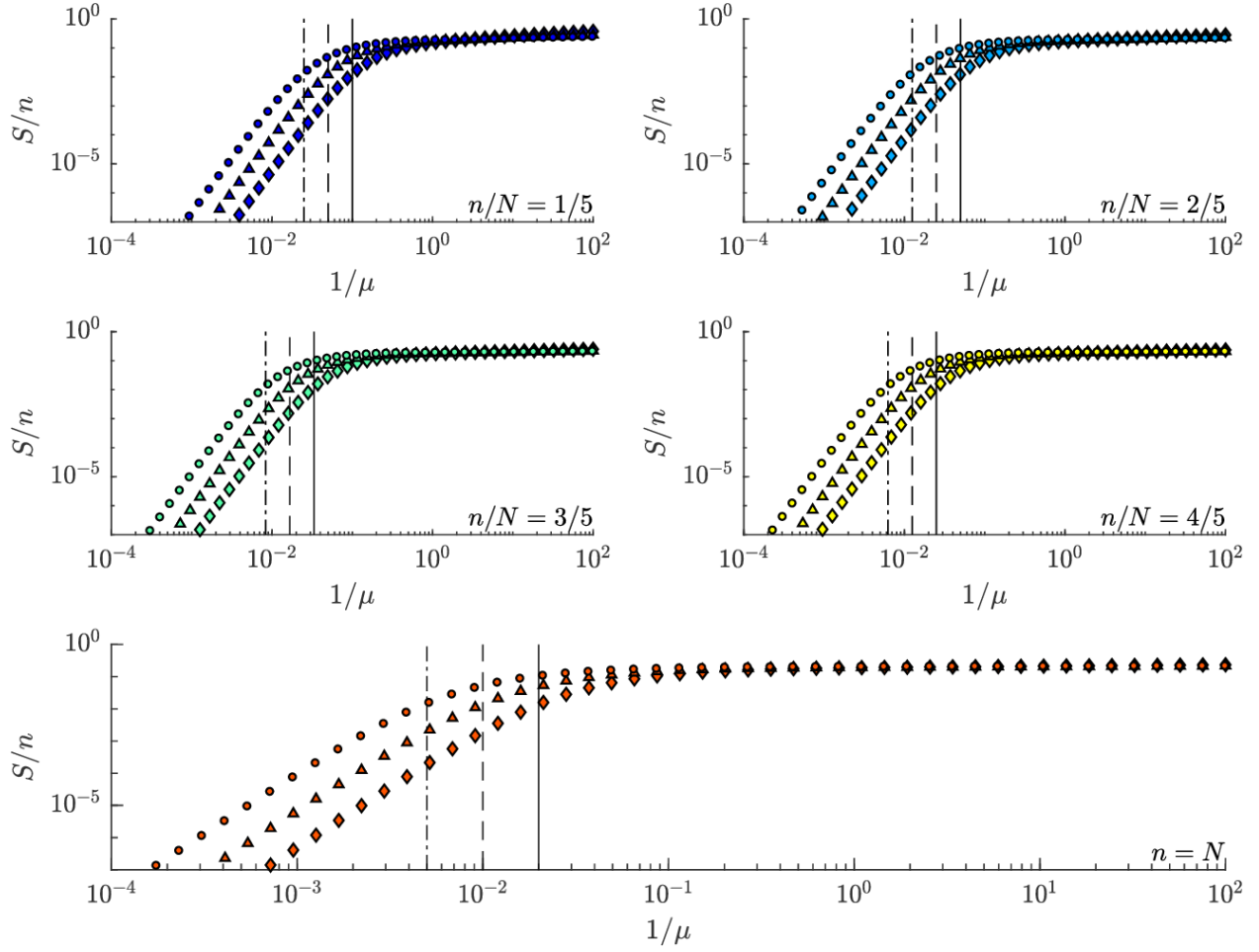
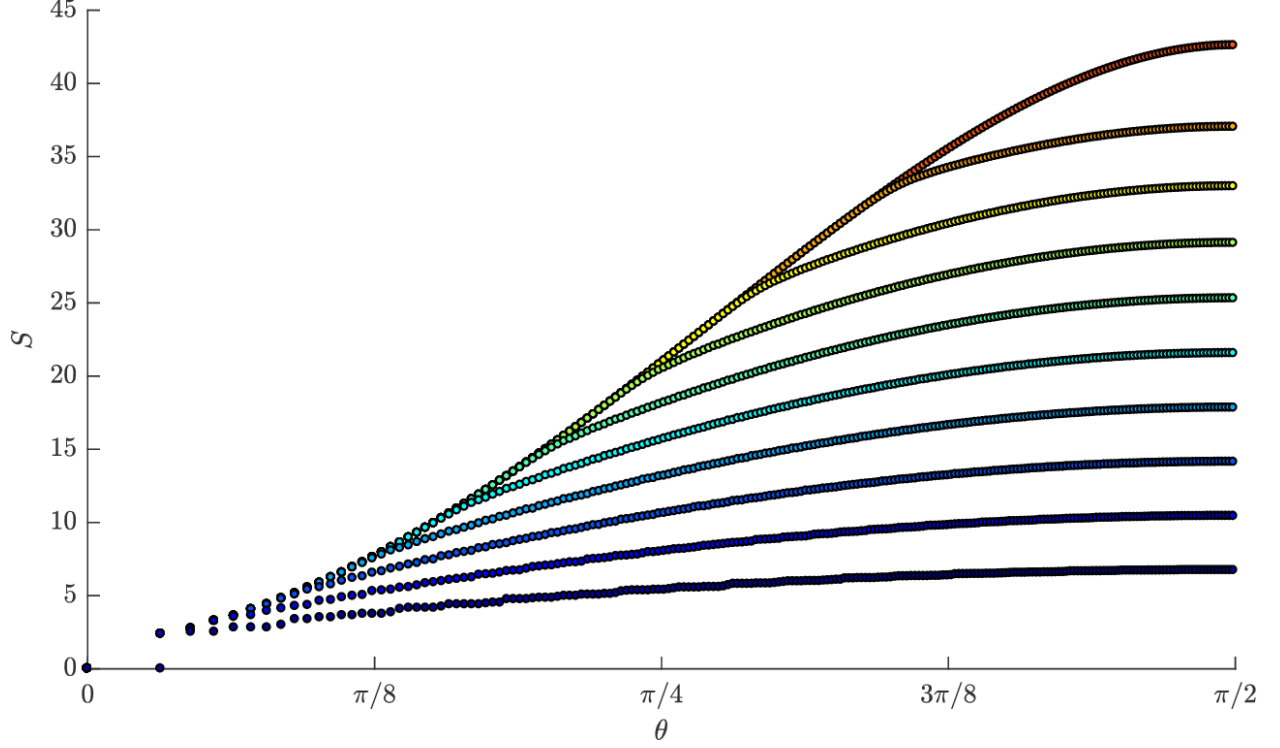
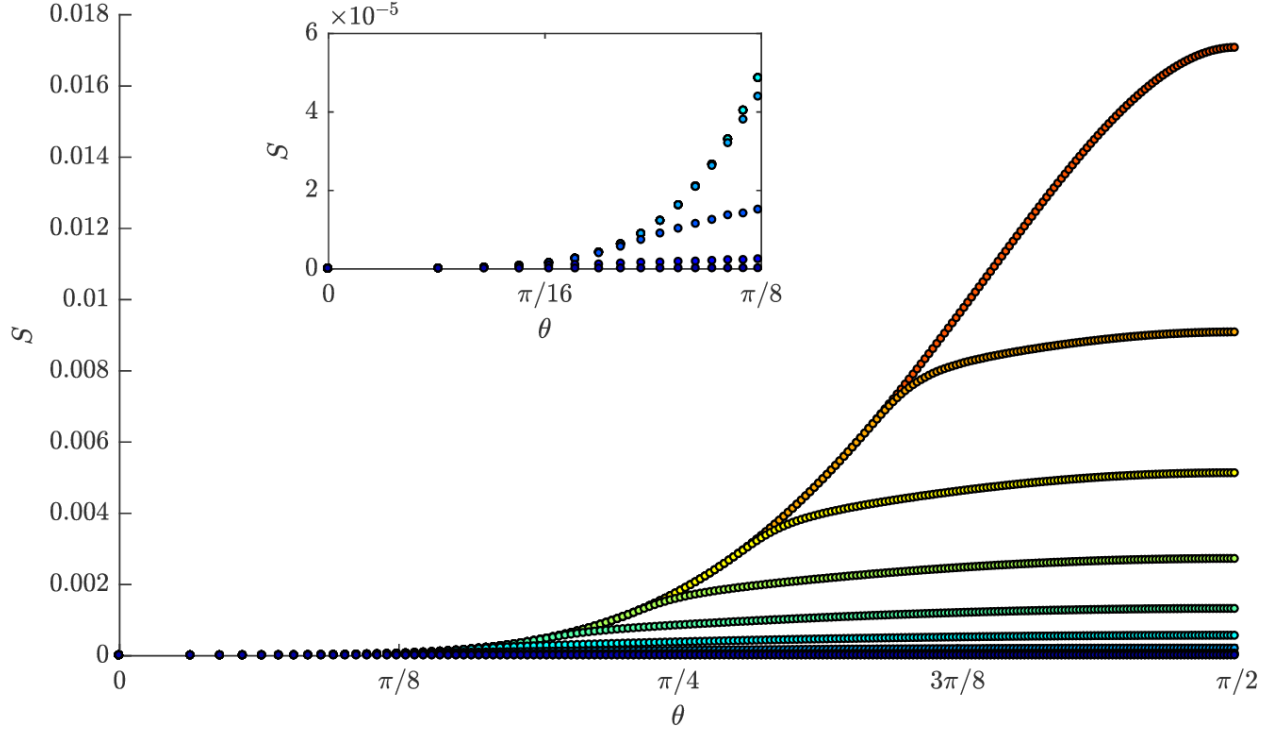


Figure 5: Scaled entropy S/n of a hemisphere plotted against $1/\mu$ for various UV cutoffs and various N . The UV cutoffs correspond to $n = N/5, 2N/5, \dots, N$, as indicated. Large diamonds, medium triangles, and small circles indicate $N = 50, 100$ and 200 , respectively. Corresponding to those values of N , the solid, dashed, and dash-dotted lines mark $\mu = n$.



(a) $\mu = 1/1000$



(b) $\mu = 1000$

Figure 6: Entropy S of a spherical cap as a function of θ for $N = 200$ with (a) a small mass $\mu = 1/1000$ and (b) a large mass $\mu = 1000$. UV cutoff parameters are $n = 20, 40, \dots, 200$ indicated with colors from dark blue to redish orange.

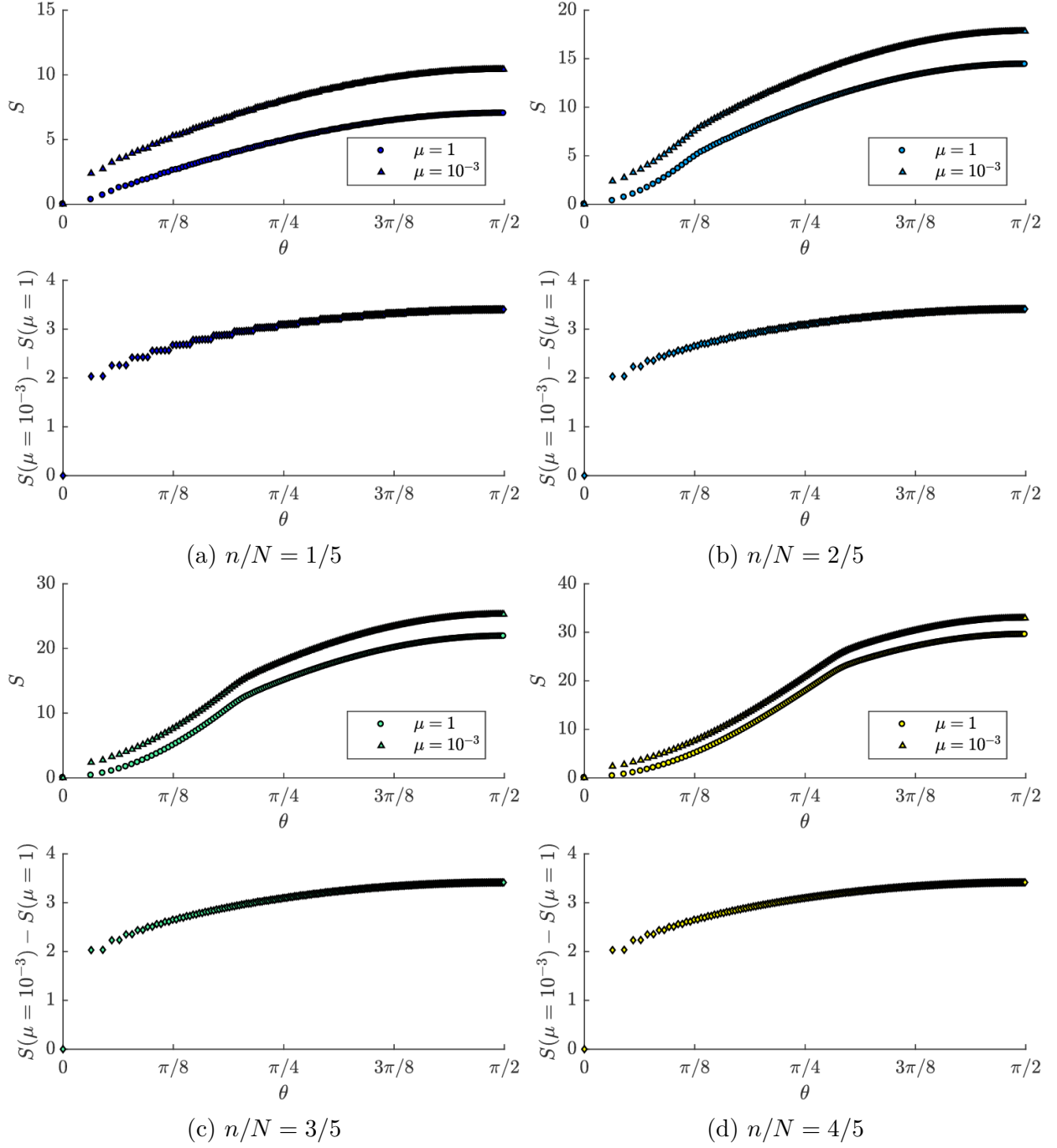


Figure 7: Entanglement entropies with $\mu = 1$ and $\mu = 10^{-3}$ and their difference as a function of θ , for various values of the UV cutoff parameter n . $N = 200$.

4 Mutual Information

Another quantity that behaves in an interesting way in strongly coupled theories [7] is mutual information. Mutual information is a useful quantity to study because it is UV finite and—perhaps because of that—is the same on the fuzzy sphere as it is on the ordinary sphere [10]. Given this, we compute mutual information to validate our choice of method for the assignment of degrees of freedom.

Mutual information is defined for a pair of regions. Taking those to be two polar caps C_1 and C_2 centered at opposite poles of the sphere, mutual information is given by

$$I = S(C_1) + S(C_2) - S(C_1 \cup C_2) .$$

To be able to compute it, we need to be able to assign degrees of freedom (subspaces of $V_n^{(m)}$) to caps C_1 and C_2 as well as their union $C_1 \cup C_2$. One condition we must impose is that the linear subspace associated with C_1 must be orthogonal to the linear subspace associated with C_2 ; otherwise, we would have a situation where two functions, despite of having support on just one of two disjoint regions, have a non-zero overlap. This can be easily and naturally achieved with the operator $Z_n^{(m)}$ defined in section 2. Given angular sizes θ_1 and θ_2 of the two spherical caps C_1 and C_2 (with θ_2 measured from the south pole), we have $z_1 = (N - \frac{1}{2}) \cos \theta_1$ and $z_2 = -(N - \frac{1}{2}) \cos \theta_2$. Degrees of freedom within C_1 are given by eigenvectors of $Z_n^{(m)}$ with eigenvalues greater than z_1 and degrees of freedom within C_2 are given by eigenvectors of $Z_n^{(m)}$ with eigenvalues less than z_2 . Because these eigenvectors are mutually orthogonal, $C_1 \cup C_2$ can be simply associated with the direct sum of these two subspaces.

For simplicity, we compute mutual information $I(N, n; \theta)$ when the two polar caps C_1 and C_2 have the same angular size θ . Following our notation for entanglement entropy, we denote mutual information on a commutative sphere with $I(\infty, n; \theta)$. In [10] it was shown that $I(n, n; \theta)$ is independent of n and that $I(n, n; \theta) = I(\infty, n; \theta)$. Given this, we would expect that $I(N, n; \theta)$ would be independent of n over the entire range of $N \in [n, \infty)$. This is indeed what is seen in Figure 8: mutual information seems unaffected by the cutoff, except for some artifacts having to do with discretization of the angle θ , which should go away at large N . This fact is further evidence that our prescription for identifying degrees of freedom associated with spherical cap regions works. Mutual information turns out to be a nontrivial test for the validity of degree of freedom assignment. In the remainder of the paper, we discuss different approaches to this assignment and explain why they appear to be inadequate.

In section 2 we defined a nearly-projection operator $P_{\theta, n}^{(m)} := O_n^{(m)} P_\theta^{(m)} (O_n^{(m)})^T$. We now define¹ $P_1 := O_n^{(m)} P_{\text{north}, \theta_1}^{(m)} (O_n^{(m)})^T$ and $P_2 := O_n^{(m)} P_{\text{south}, \theta_2}^{(m)} (O_n^{(m)})^T$ and try to associate eigenvectors of P_1 and P_2 with eigenvalues greater than half with degrees of freedom of the corresponding spherical cap. Unfortunately, while the associated subspaces are linearly

¹Omitting indices at this point to reduce clutter.

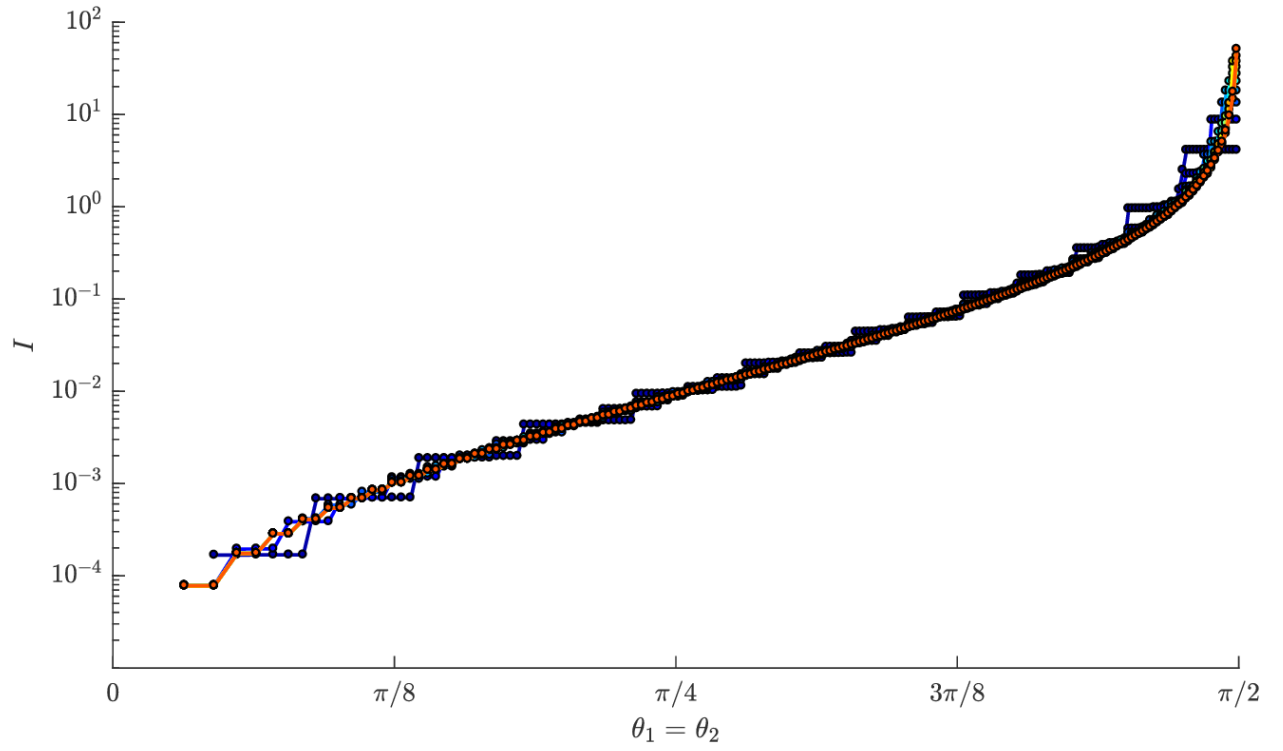


Figure 8: Mutual information $I(N, n; \theta)$ as a function of common angular size $\theta = \theta_1 = \theta_2$ of two spherical caps centered at opposite poles of the sphere. $N = 200$ and $\mu = 1$. Colors ranging from dark blue to redish orange represent UV cutoff parameter $n = 20, 40, \dots, 200$.

independent vector spaces,² they are not guaranteed to be orthogonal. In addition to re-assigning degrees of freedom slightly to fix this, we also need to make sure that the vector space associated with $C_1 \cup C_2$ is the direct sum of vector spaces associated with C_1 and C_2 . This requirement introduces an ambiguity, because there are degrees of freedom that do not appear to correspond to C_1 or C_2 , but which could reasonably be thought of as belonging to $C_1 \cup C_2$.³ We can choose to associate a direct sum of vector spaces associated with C_1 and C_2 as the vector space associated with $C_1 \cup C_2$. We call this the ‘exclusive’ method as it appears to include the smallest possible number of degrees of freedom with $C_1 \cup C_2$. An alternative is an ‘inclusive’ method, where we first fix the vector space associated with $C_1 \cup C_2$ as the span of eigenvectors of $P_1 + P_2$ with eigenvalues greater than half, and then decide how to break this vector space into a sum of two pieces associated with C_1 and C_2 respectively. This second method includes more degrees of freedom in $C_1 \cup C_2$ than the first. In either of the two cases, it is necessary to decide how to break a vector space into two pieces associated with either spherical cap. We do this by examining the eigenvectors of $P_1 - P_2$ (restricted to the space associated with $C_1 \cup C_2$). Those associated with positive eigenvalues we assign to cap C_1 and those associated with negative eigenvalues we assign to cap C_2 . Notice that if there is no UV cutoff imposed ($n = N$), P_1 , P_2 and $P_1 + P_2$ are projection operators, none of the above ambiguities arise and both methods reduce to that using $Z_n^{(m)}$.

Not only are the assignment methods based on P_1 and P_2 much more complicated than the one based on $Z_n^{(m)}$, using them yields different results for mutual information. Artifacts appear in mutual information $I(N, n; \theta)$ for θ larger than the transition θ_{trans} . Those artifacts are UV finite in the exclusive assignment method and grow like N in the inclusive assignment method. It would be interesting to understand further why out of several superficially similar methods for assigning degrees of freedom, only one leads to sensible mutual information.

Acknowledgments

This work was completed with support from the Natural Sciences and Engineering Council of Canada (NSERC), grant SAPIN-2016-00032.

²This is easy to show. Let v be any normalized linear combination of eigenvectors of P_1 with an eigenvalue greater than half. Then, $v^T P_1 v > \frac{1}{2}$. Since $\text{Id}_{V_m} - P_{\theta_1} - P_{\theta_2}$ is obviously a positive semidefinite operator, $\text{Id}_{V_m} - P_1 - P_2$ is also a positive semidefinite operator. Therefore, $v^T P_2 v < \frac{1}{2}$ and v cannot be a linear combination of eigenvectors of P_2 with an eigenvalue greater than half.

³ Consider that there might exist a normalized vector v in $V_n^{(m)}$ such that $v^T P_1 v < \frac{1}{2}$ and $v^T P_2 v < \frac{1}{2}$, but $v^T (P_1 + P_2) v > \frac{1}{2}$.

References

- [1] S. Ryu and T. Takayanagi, *Holographic derivation of entanglement entropy from AdS/CFT*, *Phys.Rev.Lett.* **96** (2006) 181602, [[hep-th/0603001](#)].
- [2] W. Li and T. Takayanagi, *Holography and Entanglement in Flat Spacetime*, *Phys.Rev.Lett.* **106** (2011) 141301, [[arXiv:1010.3700](#)].
- [3] M. Edalati, W. Fischler, J. F. Pedraza, and W. Tangarife Garcia, *Fast Scramblers and Non-commutative Gauge Theories*, *JHEP* **1207** (2012) 043, [[arXiv:1204.5748](#)].
- [4] J. L. Barbon and C. A. Fuertes, *A Note on the extensivity of the holographic entanglement entropy*, *JHEP* **0805** (2008) 053, [[arXiv:0801.2153](#)].
- [5] J. L. Barbon and C. A. Fuertes, *Holographic entanglement entropy probes (non)locality*, *JHEP* **0804** (2008) 096, [[arXiv:0803.1928](#)].
- [6] W. Fischler, A. Kundu, and S. Kundu, *Holographic Entanglement in a Noncommutative Gauge Theory*, *JHEP* **01** (2014) 137, [[arXiv:1307.2932](#)].
- [7] J. L. Karczmarek and C. Rabideau, *Holographic entanglement entropy in nonlocal theories*, *JHEP* **10** (2013) 078, [[arXiv:1307.3517](#)].
- [8] D. Dou and B. Ydri, *Entanglement entropy on fuzzy spaces*, *Phys.Rev.* **D74** (2006) 044014, [[gr-qc/0605003](#)].
- [9] J. L. Karczmarek and P. Sabella-Garnier, *Entanglement entropy on the fuzzy sphere*, *JHEP* **03** (2014) 129, [[arXiv:1310.8345](#)].
- [10] P. Sabella-Garnier, *Mutual information on the fuzzy sphere*, *JHEP* **02** (2015) 063, [[arXiv:1409.7069](#)].
- [11] P. Sabella-Garnier, *Time dependence of entanglement entropy on the fuzzy sphere*, *JHEP* **08** (2017) 121, [[arXiv:1705.0196](#)].
- [12] C. Rabideau, *Perturbative entanglement entropy in nonlocal theories*, *JHEP* **09** (2015) 180, [[arXiv:1502.0382](#)].
- [13] S. Okuno, M. Suzuki, and A. Tsuchiya, *Entanglement entropy in scalar field theory on the fuzzy sphere*, *PTEP* **2016** (2016), no. 2 023B03, [[arXiv:1512.0648](#)].
- [14] M. Suzuki and A. Tsuchiya, *A generalized volume law for entanglement entropy on the fuzzy sphere*, *PTEP* **2017** (2017), no. 4 043B07, [[arXiv:1611.0633](#)].
- [15] L. Bombelli, R. K. Koul, J. Lee, and R. D. Sorkin, *A Quantum Source of Entropy for Black Holes*, *Phys. Rev.* **D34** (1986) 373–383.

- [16] M. Srednicki, *Entropy and area*, *Phys.Rev.Lett.* **71** (1993) 666–669, [[hep-th/9303048](#)].
- [17] S. Minwalla, M. Van Raamsdonk, and N. Seiberg, *Noncommutative perturbative dynamics*, *JHEP* **0002** (2000) 020, [[hep-th/9912072](#)].